A ROUTINE TO GENERATE A SIMPLIFIED DYNAMIC MODEL OF WING MAIN BOX

Guilherme Ciscone Bufeli, guilhermebufeli@gmail.com
Alessandro Teixeira Neto, ale.teixeira@zipmail.com.br
Flávio Luiz de Silva Bussamra, flaviobu@ita.br
ITA - Instituto Tecnológico de Aeronáutica
Divisão de Engenharia Aeronáutica
Praça Marechal Eduardo Gomes, 50 - Vila das Acácias
CEP 12.228-900 – São José dos Campos – SP – Brazil

Abstract. *This work presents a routine to build a simplified model for a wing main box sized through an optimization tool for structural stability. This simplified model must represent dynamically the main box behavior. The methodology is applied to a 34m-wingspan conceptual commercial transport aircraft. Finite elements models are built in order to validate the proposed methodology. The implemented routine generates results with the expected accuracy for the preliminary sizing stages of aircrafts.*

Keywords: *structures, dynamics, buckling, structural optimization.*

1. INTRODUCTION

Nowadays the aeronautic industry seeks after the assembly of multidisciplinary tools that aid the generation of aerodynamic, aeroelastic and structural parameters the most optimized as possible. Therefore optimization tools are adapted to some from other discipline or new modules are created and integrated to each other. Based on the ideas above, this work aims the development and integration of a new routine in the optimization tool for structural stability conceived by Rissardo (2006). The new routine output is a FEM model that represents dynamically the structure generated under stability criteria.

2. WING STRUCTURAL STABILITY PRE-SIZING METHODOLOGY

Rissardo (2006) presents the development of a pre-sizing tool for wing boxes based on a new proposal for optimum integral reinforced flat panels. Bruhn (1973) presents the theoretical basis for torsion and structural stability. Niu (1999) presents the basics of structural components design. Megson (2007) and Bismarck (1999) presents the simplified formulation of aeroelasticity.

2.1. Integral Panels Optimization Model

Rissardo (2006) started with the work which Neto (2005) presented a new methodology for flat panels under compression using as stability failure criteria the following: Column Buckling, Panel Web Buckling, Stringers Local Buckling and Crippling. The major results of this work are: variables relation is constant for any length L, the critical load is constant independently from the geometry and is about 2/3 of the yield stress of the material employed and the critical load can be a function of the length of the panel. Fig. 1 shows the geometry of the reinforced panel.

Neto (2006) also demonstrated that the optimum geometry is achieved when the four critical loads take the same value, meaning that the earlier solution is just one that maximizes the stress allowable and minimizes the structure weight. For any b_s/L relation (Fig. 1) there is a set of relations that defines the optimum panel, as in Tab. 1.

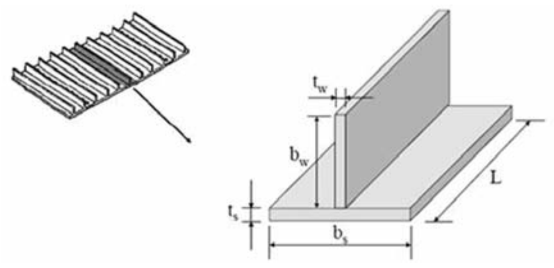

Figure 1 – Integral reinforced panel basic geometry.

Table 1 – Parametric optimization results, Neto (2005).

b_s / L	b_w / b_s	t_s / b_s	t_w / t_s	P_c / L^2
0.1832	0.3684	0.03256	1.1480	0.43224

2.2. Proposed Methodology

The developed routine uses the pre-sizing tool from Rissardo (2006), and generates a simplified Finite Element (FEM) bar model that represents dynamically a wing main box and also calculates the divergence speed. The sizing sequence is the following: initially the equivalent rectangular section is calculated in order to represent a rib bay through a bar finite element, then the shear centers that define the elastic axis are determined. These shear centers are also the nodes locations that define those bar elements. The concentrated masses that simulate each rib bay are positioned in the mass center of each bay. Finally, the divergence speed is calculated. Figure 2 presents the steps added in the pre-sizing tool.

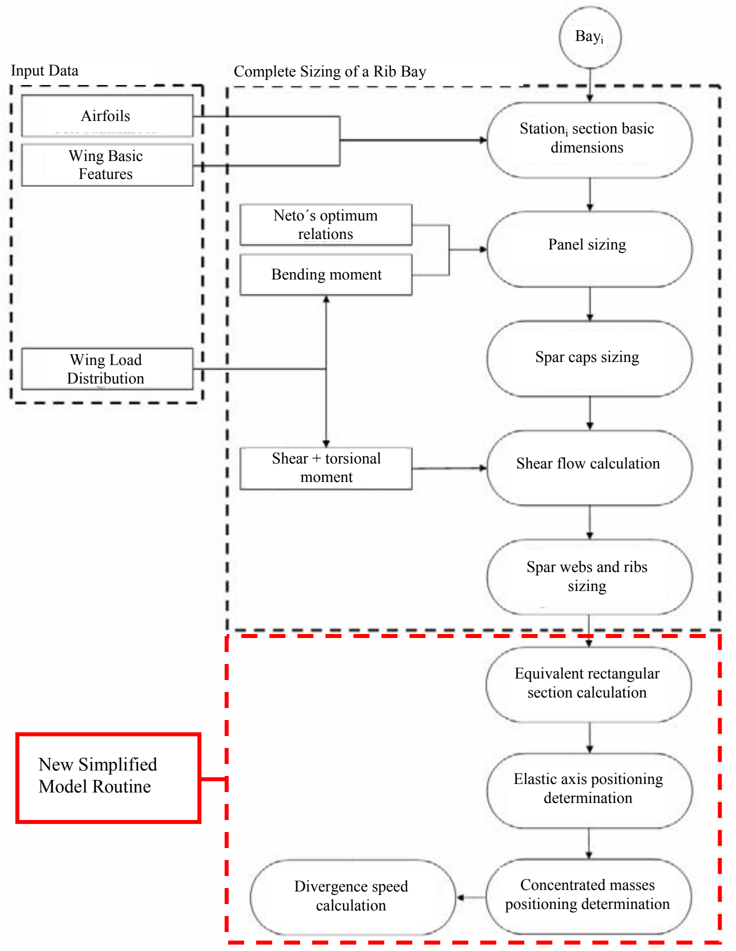

Figure 2 – Rib bay sizing representation.

The tool assumes some simplifications and hypotheses in the geometric model. One of them is to consider that the rear spar do not have a kink near the root. The third spar is not considered. The ribs are perpendicular to the line defined by the average points between the two spars. Figure 3 exemplifies the main box typical section. It is also assumed that the section is symmetrical to the x axis.

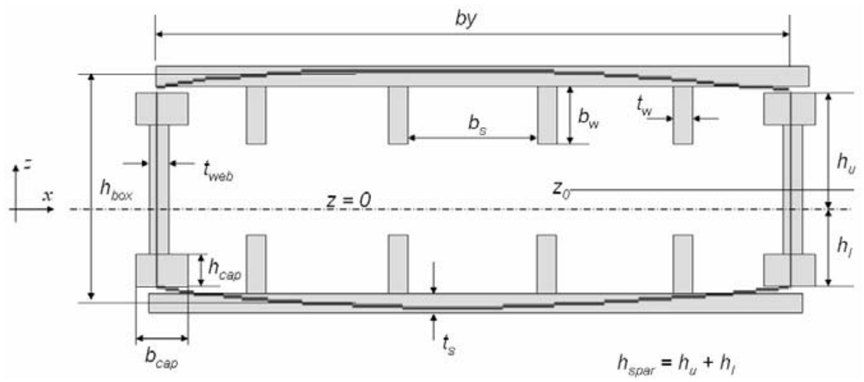

Figure 3 – Main box typical section.

Thin wall structures usually have longitudinal stringers that have opened or closed sections. According to Bruhn (1973), the torsional stiffness of the stringers is so small when compared to the one from the whole cell that can be ignored. Thus, the equation (1) can be used to calculate the polar moment inertia, J:

$$\theta = \frac{TL}{GJ} \tag{1}$$

where θ is the twist angle, T is the applied torque and G is the elastic shear modulus and transverse. Isolating J, the equation above can be rewritten as follows:

$$J = \frac{4A^2}{\oint \frac{ds}{t}} = \frac{4A^2}{\sum_{i=1}^{n} \frac{b_i}{t_i}} \tag{2}$$

where b_i e t_i are respectively the width and thickness of the wing section elements excluding the stringers.

2.3. Simplified Section Model

The simplified model has rectangular shape section with inertia moments equivalent to the ones from the wing main box pre-sized. The goal is to find the dimensions *b* and *t* that define the section described. To achieve this goal, the formulation proposed by Bruhn (1973) that relates the polar moment of inertia with the width *b* and the thickness *t,* from the simplified section presented in Fig. 4, is used.

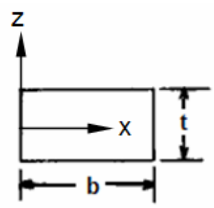

Figure 4 – Simplified model section.

This procedure could be omitted, since the bar element that represents the rib bay could be defined in a different way, but in this work the Bruhn procedure is chosen due its interesting way to relate the simplified section dimensions to the pre-sizing results for stiffness. The following formulation is the result of a mathematical elasticity analysis for maximum shear stress and torsion angle per length unit.

$$\tau_{MAX} = \frac{T}{abt^2} \tag{3}$$

$$\theta = \frac{T}{\varphi b t^3 G} \tag{4}$$

The values of a and φ are given by Tab. 2. From the above equation is obtained the polar moment of inertia of the simplified equation: The methodology used to relate the moment of inertia with b and t was an iterative algorithm described as follows. Initially, having the I_{xx} value and assuming $b = t$:

$$J = \varphi b t^3 \tag{5}$$

Table 2 – Variables a and φ as function of b/t.

b/t	1.00	1.50	1.75	2.00	2.50	3.00	4	6	8	10	∞
a	0.208	0.231	0.239	0.246	0.258	0.267	0.282	0.299	0.307	0.313	0.333
φ	0.141	0.196	0.214	0.229	0.249	0.263	0.281	0.299	0.307	0.313	0.333

$$b = (12 I_{xx})^{1/4} \tag{6}$$

At this point b/t is equal to 1 and, from Tab. 4, φ assumes the value 0,141. J is obtained using the equation (5). If this value of the polar moment of inertia is equal to the one calculated in the pre-sizing no more iterations are required. If this is not true the following steps are used: The value of b is incremented and then t is calculated: With the new relation b/t a new φ is obtained. To know this new value of φ from Tab. 4 a function of φ versus *ln(b/t)* is presented in Fig. 5.

$$t = \left(12 \frac{I_{xx}}{b}\right)^{1/3} \tag{7}$$

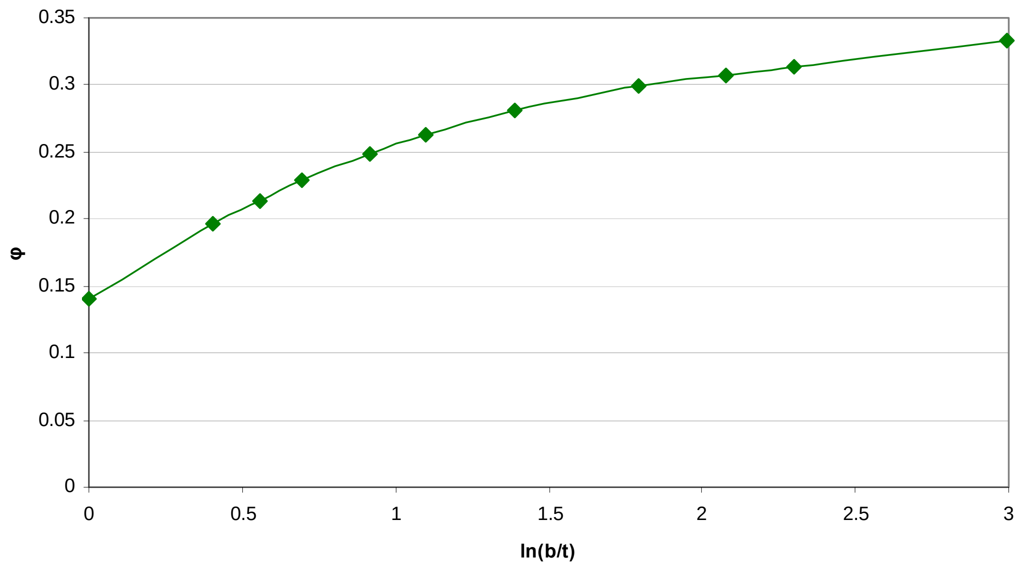

Figure 5 – Variable φ as a function of *ln(b/t)*.

Thus, with the new values of φ, b and t, a new J of the simplified section can be calculated, and then compared to the one from the pre-sizing. These iterations are repeated until the convergence is reached. After the convergence, the value of I_{zz} is calculated as consequence. As the wing main box is idealized with symmetry between the planes xy and yz it should provide a reasonable value to the purpose of representation of the dynamic behavior of the structure. Thus:

$$I_{ZZ} = \frac{tb^3}{12} \tag{8}$$

2.4. Concentrated Mass

The concentrated mass represents the mass of a single rib bay. The positioning point is defined as the average of the points that define each rib bay, adding in x direction the difference that refers to the mass center of the section.

3. PRELIMINARY DESIGN APPLICATION

Here are presented the results from the application of the previously discussed methodology. The design described below is the result of a preliminary design study of a commercial aircraft. Tab. 3 shows the main characteristics of this aircraft wing.

Table 3 – Reference wing geometry.

Reference Wing	
Aspect Ratio	9.75
Taper ratio	0.25
Angle of sweep (leading edge)	31.3º
Angle of sweep (¼ chord)	29.0º
Dihedral	2.5º
Root thickness (t/c)	14.6%
Tip thickness (t/c)	9%
Wing area (m²)	115.6
Span (m)	33.56
Chord – root (m)	5.51
Chord – tip (m)	1.37

The front spar is positioned at 13.7% of the root chord and at 20% of the chord in the tip. The rear spar is located at 58% of the root chord and at 60% in the tip. Supercritical aerodynamic profiles were adopted for this wing. The wing load employed is the one recommended by Niu (1999) to preliminary calculations which consists of the wing load distribution resultant from a pull-up maneuver with maximum load factor applied in the aircraft Center of Gravity. Table 4 shows some data from the hypothetical aircraft.

Table 4 – Mass and load factor.

Aircraft Data	
Maximum Take-off Weight (MTOW)	55,000 kg
Maximum load factor ($n_{máx}$)	2.5

The results below consider the configuration of minimum distance between ribs of 300 mm and upper/lower skins with 5 stringers. Figure 6 presents the results for ribs distance. It can be noticed that the distance between ribs diminishes from the root to the wing tip. The lower bound of the curve refers to the minimum distance defined before the sizing process. The positioning of the main components for the simplified model is presented in the Fig. 7. It is highlighted in the figure the elastic axis defined by the shear centers which are also the coordinates for the nodes of the finite bar elements. Fig. 7 also shows the concentrated masses between the ribs and over the mass center of each bay.

Concerning the ribs distribution there is a large space between them from the root until the bay 5 (y = 12290 mm) generated due the nature of the pre-sizing tool, conceived basically to solve the stability issue. In a real design case other components would be assembled to this wing (control surfaces supports, main landing gear trunnions and others) that would require the addition of new ribs. Figure 8 presents the FEM simplified model generated to obtain the structure vibration modes of the wing. The divergence speed at sea level is 1514 m/s which means it is outside the aeroelastic envelope of the hypothetic aircraft.

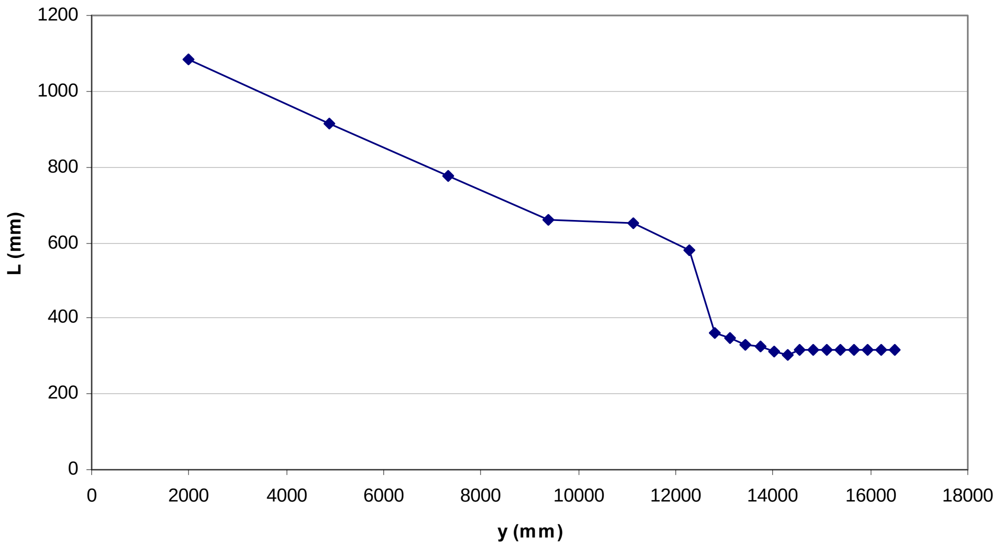

Figure 6 – Spacing between ribs variation through wing semi-span.

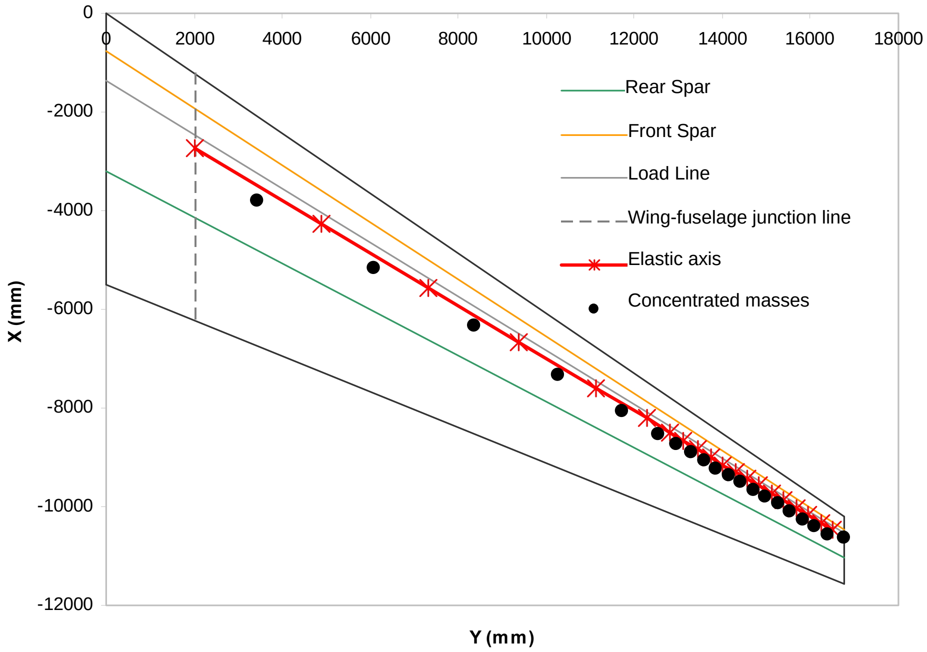

Figure 7 – Simplified model representation over the original wing geometry.

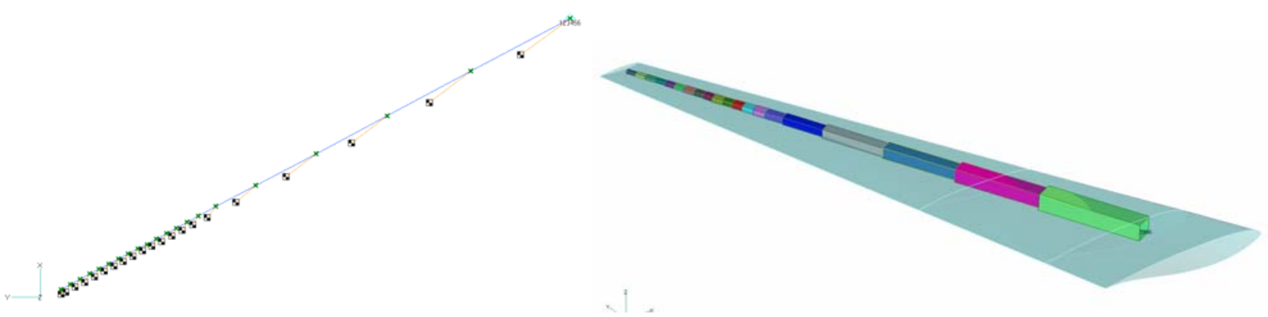

(a) (b)

Figure 8 – (a) Simplified model with its concentrated masses; (b) The bar elements sections represented.

4. ANALYSIS RESULTS AND FINITE ELEMENTS METHOD VALIDATION

A global FEM model was built to validate the wing main box results from the pre-sizing tool. The Nastran solution 105 was used to obtain the buckling modes of the structure. The simplified model was used in order to validate the normal modes of vibration. The Nastran solution 103 was used to obtain both FEM models normal modes.

4.1. Global Model

The maximum displacement in the wing tip is 1983 mm which is considered coherent for a wing with span of 33.56 meters. Figure 9-a plots the distribution of minor principal stress for upper skin and Fig. 9-b presents the distribution of major principal stress for the lower skin. The stress analysis addresses that absolute maximum values are similar, -24.1 daN/mm^2 (minor principal) and 26.3 daN/mm^2 (major principal). This can be explained by the symmetry of upper and lower panels. Table 5 presents the buckling critical loads as results of the Nastran solution 105 and the rib bay where the panel buckles. The first two modes and the 20th mode represent an overall buckling. Figure 10 presents the first buckling mode for this structure.

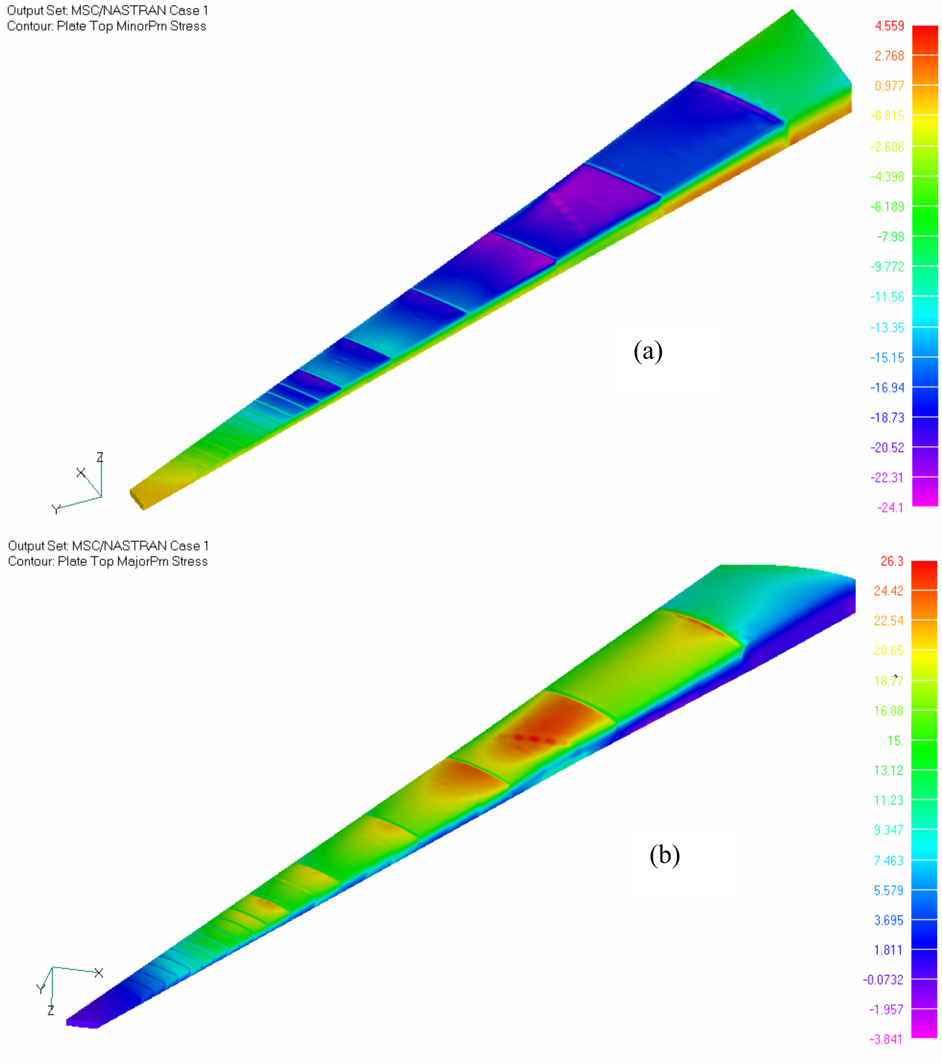

Figure 9 – (a) Minor principal stress; (b) Major principal stress.

Table 5– Critical buckling loads summary.

Mode	λ	Bay									
		1	2	3	4	5	6	7	8	9	10
1st	1.464	x	x	x	x	x	x	x	x	x	x
2nd	1.508	x	x	x	x			x	x	x	
3rd	1.560						x				
4th	1.594							x	x		
5th	1.604						x				
6th	1.608			x							
7th	1.629			x							
8th	1.669							x			

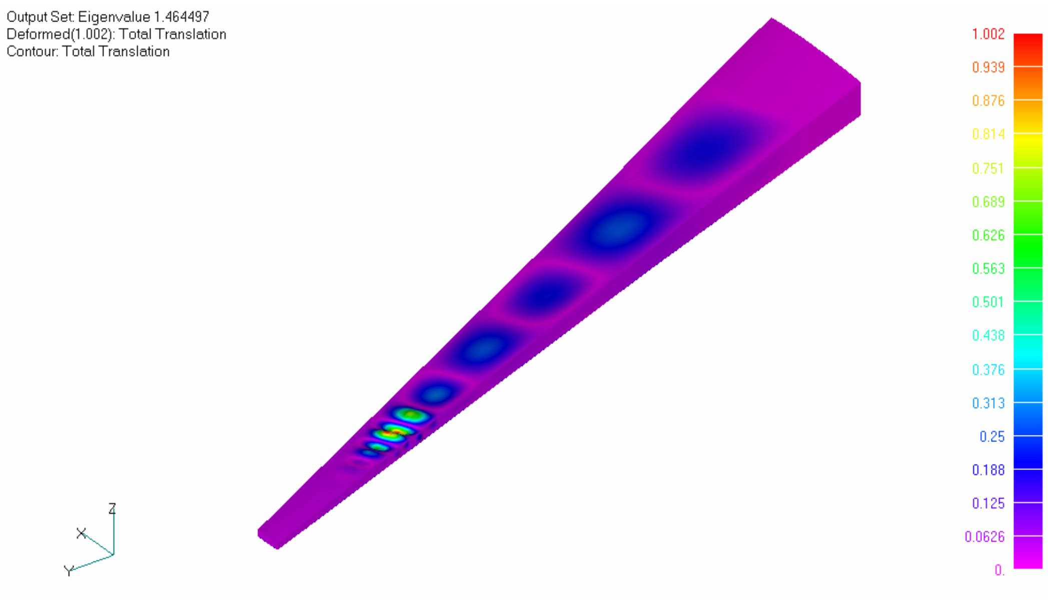

Figure 10 – First buckling mode, λ = 1.4645.

4.2. Simplified Model

The maximum displacement at the wingtip is 1750 mm, a similar value to the one found for the global model, the difference between them is 233 mm or 11.75%. The frequency values found addresses that, in general, the simplified model outputs values slightly lower for each normal mode when analyzed the results for both models in the sequence that they are given. On the other hand, when it is compared only the way that the mode behaves and not the frequency, it can be concluded that some modes emerge only from one of the FEM models. An example is the second mode from the simplified model. It does not have a similar mode from the global model and the 7th and 8th modes from global model do not have a similar normal mode from the simplified model.

The second mode from the simplified model is a bending mode towards z axis. The 7th normal mode from global model is a torsion coupled with an expansion of the wing main box. The 8th mode consists of waves formation all over the wing. These modes are presented in Fig. 11. These modes below only could be found in the global FEM model due its deformation and coupling features. Fig. 12 presents a comparison only for the modes that appears in both models. Figure 13 shows the first normal mode for both modes, first the global FEM model and then the simplified model.

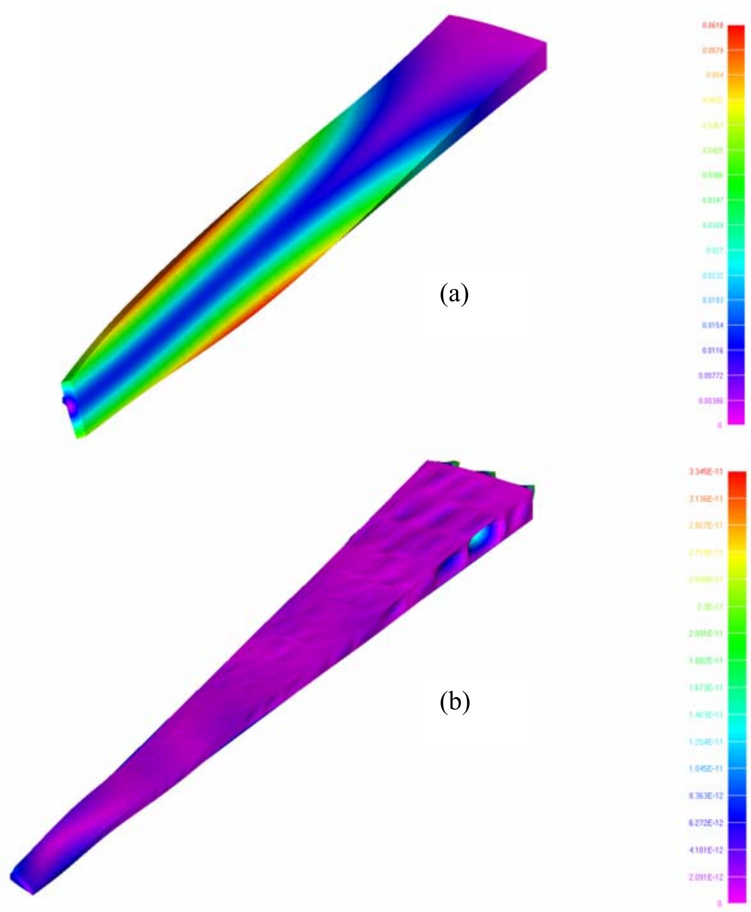

Figure 11 – (a) 7th normal mode; (b) 8th normal mode – Global FEM model.

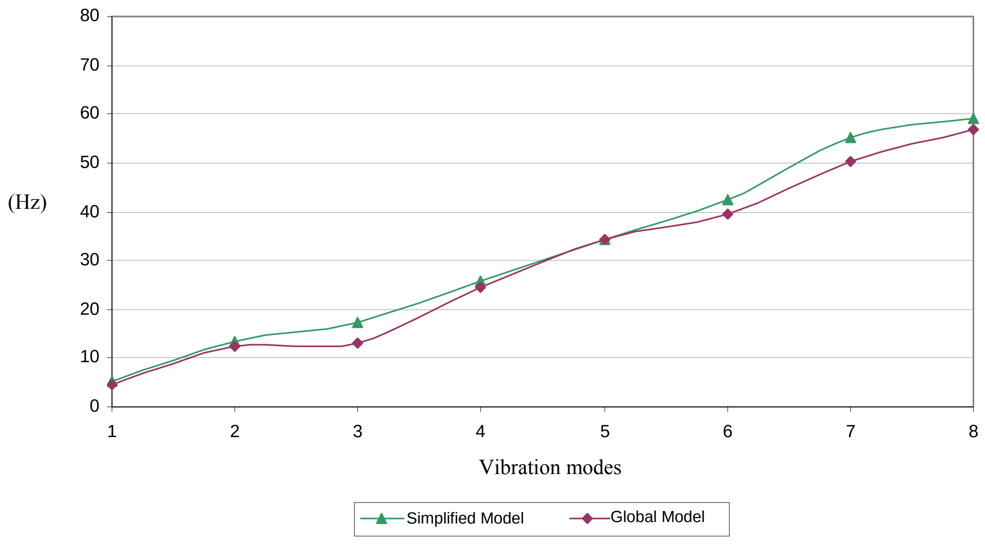

Figure 12 – Vibration modes and its frequencies.

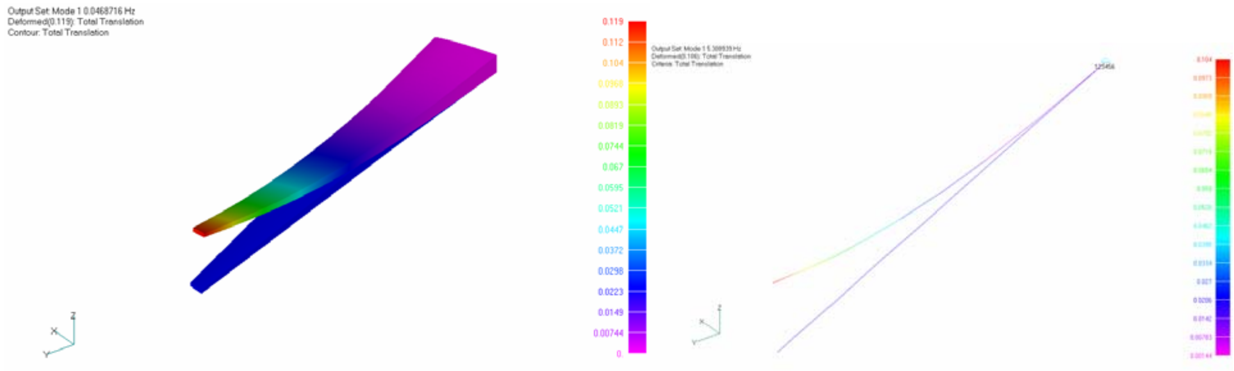

(a) (b)

Figure 13 – Normal modes: (a) 4.68 Hz; (b) 5.31 Hz.

5. CONCLUSIONS

This work added a new calculation routine to the work developed by Rissardo (2006), with a multidisciplinary approach. It was applied to a larger and heavier wing than the one from the original work, generating results with reasonable accuracy. Thus, the pre-sizing tool proved to have good potential to engineering applicability in the early phases of the structural design of wings.

The stress distribution on the upper and lower skins is, in general, homogeneous through the wingspan, demonstrating the structural efficiency of these components that basically comes from Neto (2005 e 2006). The critical buckling loads, given by the global FEM model can be considered higher than expected, due the fact that for the Nastran solution 105 is required a more refined mesh with at least 5 elements in a semi wave. Nevertheless, this does not invalidate the analysis since it was not expected values lower than 1.

The simplified model provided good results for displacements as well as for the frequencies and normal modes. The methodology employed besides its simplicity demonstrated its reliability to generate the quite representative inertia moments of the studied wing main box. The accurate positioning of the concentrated masses is also important to obtain representative results of normal modes and frequencies.

The divergence speed, which is calculated in a conservative way, takes place outside the aeroelastic envelope as expected since a swept wing acts in a way that increases the divergence speed. It is proposed the complete flutter analysis as a next step of development in order to contribute to the multidisciplinarity of this pre-sizing tool.

Also as a future work another suggestion is the addition of a maximum distance between ribs restriction. Looking at Fig. 9 it is clear that near the root, where the distance is higher, the stress distribution is not as homogeneous as in other areas of the wing. The second half of the first rib bay is oversized for stability criteria. Hence, a restriction would redistribute in a better way the stresses in the panels resulting in a lighter structure as well.

6. ACKNOWLEDGEMENTS

This work is dedicated to Professor Maher Nasr Bismarck-Nasr (in memory).

7. REFERENCES

Bismarck-Nasr, M. N., 1999, Structural Dynamics in Aeronautical Engineering AIAA Education Series, São José dos Campos, Brasil.

Bruhn, E. F., 1973, Analysis and Design of Flight Vehicle Structures Purdue: Jacobs Pub.

Megson, T.H.G., 2007, Aircraft Structures for Engineering Students Butterworth-Heinemann.

Neto, A. T, 2005, Parametric Optimization of Integrally Machined Panels Regarding Four Stability Criteria Proceedings of 18th COBEM International Congress of Mechanical Engineering.

Neto, A. T., 2006, Parametric Optimization of Integrally Machined Panels Regarding Four Stability Criteria – Generalized Solution Anais do IV CONEM Congresso Nacional de Engenharia Mecânica.

Niu, M. C. Y., 1999, Airframe Structural Design 2.ed. Hong Kong: Hong Kong Conmilit Press LTD.

Rissardo, W., 2006, Uma Metodologia de Pré-Dimensionamento para a Estabilidade Estrutural de Asas, Dissertação de Mestrado – Instituto Tecnológico de Aeronáutica, São José dos Campos, Brasil.

8. RESPONSIBILITY NOTICE

The authors are the only responsible for the material included in this paper.